ELSEVIER Solar Energy Materials and Solar Cells 52 (1998) 261–269

Solar Energy Materials & Solar Cells

Analysis of the interband transitions in porous silicon

M.R. Beltrán[a,*], M. Cruz[a,b], C. Wang[a], J. Tagüeña-Martínez[c]

[a] *Institute de Inv. en Materiales, UNAM, A.P. 70-360, 04510 D.F., Mexico*
[b] *Escuela Superior de Ingeniería Mecánica y Eléctrica - UC, IPN, Mexico*
[c] *Centro de Investigación en Energí, UNAM, A.P. 34, 62580 Temixco, Mor., Mexico*

Received 1 October 1996; received in revised form 20 May 1997

Abstract

Porous silicon (PS) presents interesting phenomena such as efficient luminescence and a peculiar transport of carriers. Due to its possible optoelectronic applications, it is important to calculate the dielectric function from interband optical transitions in PS to include quantum effects. In this work, we apply a supercell model for PS within an sp^3s^* tight-binding technique, to analyze the effects of pores on the above-mentioned transitions. The polarized light absorption is studied by observing the oscillator strength behavior within two different schemes, which are applied and compared. We have found a significant enlargement of the optically active zone in the $\boldsymbol{k}$-space, due to the localization of the wave function. The calculated dielectric functions for crystalline silicon and PS are compared with experimental results, giving the correct energy range and shape.

Keywords: Porous silicon; Luminescence; Carrier transport

1. Introduction

Porous silicon (PS) is becoming an important option for optoelectronic devices due to its photo- and electro-luminescent properties. In particular, applications in highly sensitive fast photodiodes [1,2], and solar cells [3] are studied. Although photoconductivity and photovoltaic properties are observed in PS [4], PS has been used as an

* Corresponding author.

0927-0248/98/$19.00
PII S0927-0248(97)00241-9

antireflection coating for polycrystalline silicon solar cells [5]. This application is based on the extremely high ratio of surface to volume presented in PS, which enhances light trapping and reduces reflection losses. Besides this, its wide band gap makes it a candidate to optimize the sunlight absorption. Finally, PS has the technological importance of being easy to produce at low cost and most important, it is compatible with silicon micro-electronics [6]. From the theoretical point of view, the basic understanding of the efficient luminescent phenomenon has also stimulated great interest, since it is well known that crystalline silicon has an indirect band gap of 1.1 eV, which prevents efficient interband radiative recombination in the visible region.

Efforts have been made to explain the light emission from PS. At the moment there are two models explaining the mechanisms involved in the luminescence process. One of them emphasizes the quantum confinement effect [7–9] and others suggest the essential participation of the localized surface states in the silicon nanostructures [10]. However, in this work we are interested in modeling the optical properties of porous silicon, which are fundamental in the above-mentioned applications. All the quantum-mechanical theoretical works, from the Hamiltonian's choice point of view, can be classified in two major categories: first principles and semi-empirical frameworks. The first-principles calculations have been performed mainly in quantum dots (clusters) [11] or quantum wires [12]. Semi-empirical or tight-binding calculations are simple enough to be applied in larger systems with complex morphologies [13]. It is worth mentioning that the use of phenomenological parameters include many-body effects, which generally are neglected in a first-principle Hamiltonian. In this work we will follow this last approach.

In Section 2 we describe the Hamiltonian and the supercell structures used in our model. In Section 3 the results are presented, and in Section 4 we give some conclusions.

2. The model

We choose a tight-binding Hamiltonian, taking advantage of its simplicity in order to study different physical properties by using large supercells. The minimum basis capable of describing an indirect band gap along the X-direction is the sp^3s^* basis. We have used Vogl et al. [14], which reproduce an 1.1 eV gap in bulk crystalline silicon. Empty columns are produced removing columns of atoms within the supercell as schematically shown in Fig. 1. Notice that within this model and pores oriented as in Fig. 1, the percolation limit is found to be around 40% porosity. As PS exhibits a very large surface mainly hydrogen passivated [7–9], we saturate the pore surface with hydrogen atoms. The Si–H bond length is taken as 1.48 Å. Since the ground-state energy of a free H atom (-13.6 eV) is so close to the s-state energy level of a free Si atom, -13.55 eV [15], the on-site energy of H is taken to be -4.2 eV, as that of silicon [16]. The H–Si orbital interaction parameters are taken as $ss\sigma_{H\text{-}Si} = -4.075$ eV, $sp\sigma_{H\text{-}Si} = 4.00$ eV, which are obtained by fitting the energy levels of silane [11]. The porosity is measured as the ratio of the PS mass over the original crystalline silicon mass.

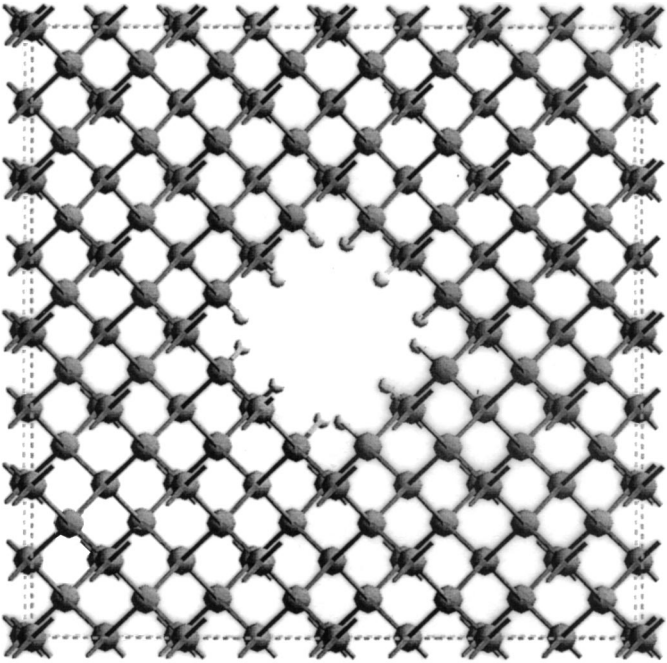

Fig. 1. Schematic representation of a 128-atom supercell used to model PS with a 9-atom columnar pore saturated with 12 hydrogen atoms per layer. Periodic boundary conditions are used in the X, Y and Z directions.

In order to analyze the effects of porosity, columns of equal shapes varying their size in 128-atom supercells are used. The electronic band calculation shows that the band gap broadens and the conduction band minimum shifts towards the Γ point, producing an almost direct band gap, as the porosity increases [13].

Apart from providing valuable information on the electronic behavior, the electronic structure calculations are a key factor for the study of optical properties through the oscillator strength analysis [17,18]. The interband oscillator strength can give some insight on the controversy of having an indirect gap in PS as it is suggested by induced absorption experiments [6], even when high luminescence efficiency is observed. Here, we will define the dimensionless interband oscillator strength following Koiller et al. [17]:

$$f_{v,c} = \frac{2}{m} |\langle v|\boldsymbol{p}|c\rangle|^2/(E_c - E_v), \tag{1}$$

where $|v\rangle$ and $|c\rangle$ are valence and conduction-band eigenstates, respectively. In the tight-binding scheme eigenstates $|e\rangle = \sum_{i,\mu} a^e_{i,\mu} |i, \mu\rangle$, where i is the site index and μ identifies the orbital, then the dipole matrix in Eq. (1) can be expressed as

$$\langle v|\boldsymbol{p}|c\rangle = \sum_{i,j,\mu,\nu} a^{v*}_{i,\mu} a^c_{j,\nu} \langle i\mu|\boldsymbol{p}|j\nu\rangle. \tag{2}$$

The dipole matrix elements in Eq. (2) may be rewritten in terms of the Hamiltonian (H) and the position ($\boldsymbol{r}$) operators, using the commutation relation $\boldsymbol{p} = im/\hbar[H, \boldsymbol{r}]$,

$$\langle i\mu|\boldsymbol{p}|jv\rangle = \frac{im}{\hbar}\sum_{l,\lambda}(\langle i\mu|H|l\lambda\rangle\langle l\lambda|\boldsymbol{r}|jv\rangle - \langle i\mu|\boldsymbol{r}|l\lambda\rangle\langle l\lambda|H|jv\rangle). \tag{3}$$

Since the polarizability of a free atom is much smaller than that of the corresponding semiconductor [19], Eq. (3) can be simplified as [17]

$$\langle i\mu|\boldsymbol{p}|jv\rangle = \frac{im}{\hbar}\langle i\mu|H|jv\rangle\boldsymbol{d}_{i,j}\,, \tag{4}$$

where $\boldsymbol{d}_{i,j} = \langle jv|\boldsymbol{r}|jv\rangle - \langle i\mu|\boldsymbol{r}|i\mu\rangle$ is the distance between centers of gravity of the orbitals μ and v placed at atoms i and j, respectively, and it is not dependent on orbitals if the crystal field is symmetric. Notice that the contribution to the dipole matrix coming from two orbitals at the same atom is neglected.

Another interesting approach to study optical properties due to Selloni et al. [18], which is widely accepted to study silicon, only retains two intra-atomic matrix elements of $\boldsymbol{r}$ in Eq. (3),

$$\langle s|x|p_x\rangle = 0.27\ \text{Å} \quad \text{and} \quad \langle s^*|x|p_x\rangle = 0.108\ \text{Å}. \tag{5}$$

These two schemes consider rather different contributions. While the first scheme (Eq. (4)), which has been used to study direct to indirect band gap transitions, emphasizes the importance of bulk participation, in the second approach (Eq. (5)) the atomic contributions are the relevant ones and it has been used in the study of surface optical properties.

The next stage in the calculation is to include all the interband transitions between the valence and the conduction band states, taking into account also the oscillator strength for non-vertical transitions in order to obtain the dielectric function ($\varepsilon = \varepsilon_1 + \mathrm{i}\varepsilon_2$). Actually, the imaginary part of the dielectric function is proportional to the sum [15]

$$\varepsilon_2 \propto \sum_{k,k'} f_{k,k'}\delta(\varepsilon_{k'} - \varepsilon_k - \hbar\omega)\,, \tag{6}$$

where $f_{k,k'}$ are the oscillator strengths defined in Eq. (1), k and k' correspond to the valence and the conduction band states, respectively.

Optical studies of solids reflect the details of the electronic structure. In particular, the dielectric function measures their response to an electromagnetic field, and its imaginary part gives the absorption properties. As we are interested in analyzing the nature of the energy band gap, this could be studied by looking at the behavior of the absorption spectrum around the band gap.

3. Results and discussion

The non-vertical interband oscillator strength between the degenerate states at the top of the valence band and those at the conduction band close to the optical gap, for

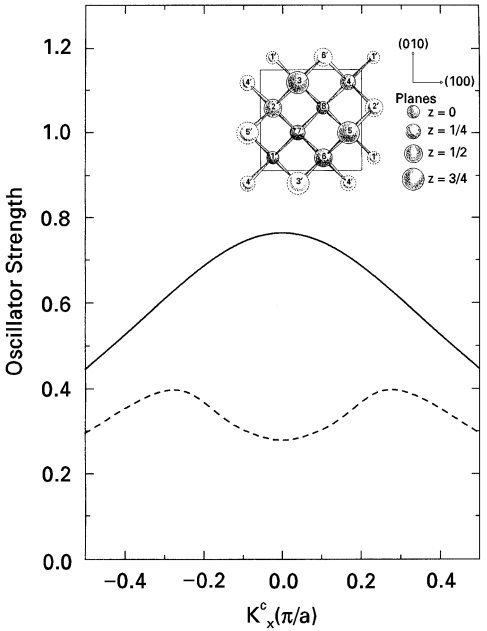

Fig. 2. The optical-gap oscillator strength calculated in eight-atom supercells with (dashed line) and without a 1-atom columnar pore (solid line). Transitions between the top valence band states ($\boldsymbol{k}^v = 0$) and conduction-band states with $\boldsymbol{k}^c$ close to the Γ point, for light excitations polarized in the x-direction are considered. An eight-atom supercell is shown at the top right corner for clarity.

x-direction polarized light, obtained from Eq. (4) is shown in Fig. 2. They are calculated in 8-atom supercells with (dashed line) and without a 1-atom columnar pore (solid line) saturated by hydrogen atoms. An eight-atom supercell is shown in the corner for clarity. Notice first that there are two absorption maxima located off the Γ-point. This fact suggests the possibility of efficient non-vertical transitions, which could be relevant to understand the luminescence observed in PS, in spite of having an indirect gap. Furthermore, a reduction of the oscillator strength for the pore case can also be observed, due to a broadening of the optically active zone, as a consequence of the sum rule [15], $\sum_k f_{k',\,k} = 1$, where the sum is over all states, occupied as well as unoccupied. This broadening could be explained through the Heisenberg's uncertainity principle, due to the localization of the wave functions caused by extra nodes introduced with the pores, although they are still Bloch-like.

The results presented in Fig. 3 have been calculated from 128-atom supercells removing square columns of 1, 4, 9, 16, 25, 36 and 49 atoms. It shows the oscillator strength versus the porosity, where transitions between wave functions at the valence band maximum and those at the conduction band minimum are considered. One can see that there is a jump of 20 orders of magnitude predicted by both schemes Eqs. (4) and (5), when a pore is introduced. This jump is due to the fact that in supercell models not all the states at the Γ point possess wave functions with $\boldsymbol{k} = 0$ symmetry. Rather,

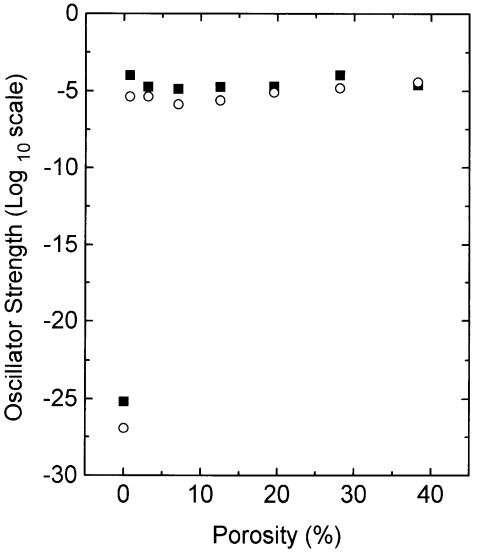

Fig. 3. Logarithm of the oscillator strength versus porosity calculated from Eq. (4) (solid squares) and Eq. (5) (open circles) explained within the text. The interband transitions are taken between the valence band maximum and the conduction band minimum in 128-atom supercells.

many are the product of the folding of the Brillouin zone, in particular, the states at the minimum of the conduction band for a 128-atom supercell. When a pore is introduced, the supercell becomes the unit cell of the system, and all Γ states are real ones, in spite of the existence of extra nodes in the wave function. After the jump, an almost constant slope is found. This fact could be explained by competing mechanisms involving the significant enlargement of the optically active zone in the $\boldsymbol{k}$-space (see Fig. 2) and the above-mentioned sum rule.

To produce Fig. 4 we have considered transitions between states of the valence band and those of the conduction band, for x-direction polarized light. They are calculated in eight-atom supercells [20] with and without columnar pores, all of which have been saturated by hydrogen atoms. Fig. 4a shows the dielectric function for crystalline silicon calculated with vertical interband transitions (solid line), i.e., $\boldsymbol{k}_i^c = \boldsymbol{k}_f^v$, and it is compared with the experimental data reported in Ref. [21] (solid circles). The calculation has been performed by considering 205,379 $\boldsymbol{k}$-points in the first Brillouin zone. It can be seen that the theory gives reasonably well the energy range and the shape, in spite that no d-orbital is considered. It is important to notice that the absorption onset (3.06 eV) corresponds to the optical c-Si gap, which is much larger than the indirect band gap (1.1 eV).

In Fig. 4b the calculated dielectric function for a supercell with a 1-atom columnar pore is shown, including non-vertical transitions, i.e., $\boldsymbol{k}_i^c \neq \boldsymbol{k}_f^v$, to consider the disorder effects in PS which have been excluded by the supercell model. The calculation has been performed only for 729 $\boldsymbol{k}$-points in the first Brillouin zone, since adding

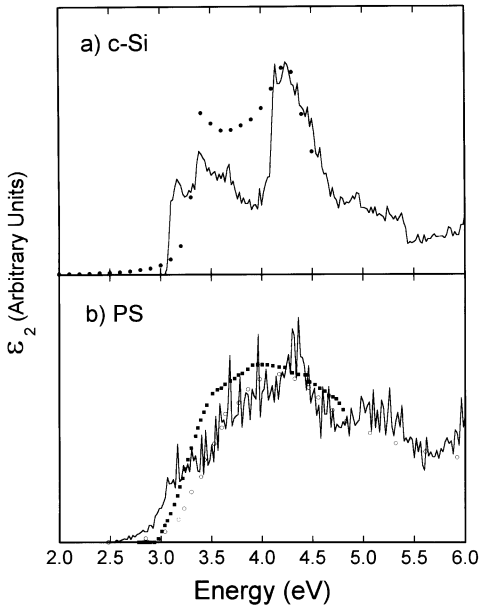

Fig. 4. Imaginary part of the dielectric function calculated in an eight-atom supercell without (solid line in a) and with (solid line in b) a 1-atom columnar pore, considering interband transitions between valence and conduction band states, for light excitations polarized in the *x*-direction. The theoretical results are compared with experimental c-Si data (solid circles in a) [21], measured PS data (solid squares in b) [23] and thin 6 Å films results (open circles in b) [22].

non-vertical transitions is a very lengthy calculation. Notice that in the calculated dielectric function a tail appears in contrast with the c-Si case. This is due to the disorder, as occurred in a-Si [22]. In our calculation this shift is produced by the relaxation of the electron wave vector conservation allowing interband transitions between states close to the almost direct band gap of 2.43 eV, in order to introduce disorder effects. Furthermore, the optically active $\boldsymbol{k}$ space is enlarged by the quantum confinement, and then the dielectric function reveals the real band gap, instead of the optical band gap. Finally, notice that a shortcoming of the model is that the porosity simulated by this supercell is only 12.5% while the experimental data are obtained from 70% porosity samples [23].

4. Conclusions

We have already mentioned the importance of technological applications of porous silicon. In particular, its optical properties could be characterized by means of physical quantities such as the dielectric function and the absorption coefficient. We have shown that a simple microscopic quantum mechanical treatment, such as a phenomenological tight-binding technique, is capable of giving essential features of the electronic behavior of PS.

First, we have found [13] that a supercell model reproduces the experimentally observed increase of the energy band gap and the appropriate shifts of the valence and conduction band edges. Furthermore, the electronic band structure shows a tendency towards a direct band gap as the porosity increases. The analysis of the oscillator strength behavior has revealed an enlargement of the optically active $\boldsymbol{k}$ zone (Fig. 2). This enlargement, together with the trend observed towards a direct band gap, could reconcile the apparent controversy between the efficient luminescence of PS and its indirect gap, observed experimentally.

It is interesting to note in Fig. 3 that although we are using substantially different schemes for the calculation of the oscillator strength, both give the same dependence with the porosity in spite of the different contributions that each one considers. Notice that the interband transitions are equally affected in both cases by the presence of pores.

Finally, from the comparison with the experimental data (Fig. 4) [22,23] of the dielectric function we can conclude that our model when non-vertical transitions are considered gives the correct energy range and shape of the PS dielectric function. The need of introducing non-vertical transitions reveals the importance of the disorder and interconnection of the silicon branches.

Acknowledgements

We acknowledge E. Sansores for his help with Fig. 1. This work has been partially supported by projects DGAPA-IN104595, CONACyT-0205P-E9506, CONACyT-4229-E, and CRAY-UNAM-SC005096.

References

[1] J.P. Zheng, C.R. Wie, Electron. Lett. 28 (1992) 911.
[2] P. Fauchet, Appl. Phys. Lett. 68 (1996) 2058.
[3] D. Dimova-Malinovska et al., Mater. Res. Soc. Symp. Proc. 405 (1996) 167.
[4] G. Stemtad, M. Kunst, C. Vial, Sol. Energy Mater. Sol. Cells 26 (1992) 277.
[5] P. Menna, G. Di Francia, V. La Ferrara, Sol. Energy Mater. Sol. Cells 37 (1995) 13.
[6] D. Lockwood, P. Fauchet (Eds.), Light Emission in Silicon Porous Silicon: Photoluminescent Devices, Semiconductors and Semimetals Series, Academic Press, New York, 1996, to appear.
[7] L.T. Canham, Appl. Phys. Lett. 57 (1990) 1046.
[8] A.G. Cullis, L.T. Canham, Nature 353 (1991) 335.
[9] L.T. Canham, M.R. Houlton, W.Y. Leong, C. Pickering, J.M. Keen, J. Appl. Phys. 70 (1991) 422.
[10] F. Koch, Mater. Res. Soc. Symp. Proc. 298 (1993) 319.
[11] F. Huaxiang, Y. Ling, X. Xie, Phys. Rev. B 48 (1993) 10978.
[12] F. Buda, J. Kohanoff, M. Parinello, Phys. Rev. Lett. 69 (1992) 1272.
[13] M. Cruz, C. Wang, M.R. Beltrán, J. Tagueña-Martínez, Phys. Rev. B 53 (1996) 3827.
[14] P. Vogl, H.P. Hjalmarson, J.D. Dow, J. Phys. Chem. Solids 44 (1983) 365.
[15] W.A. Harrison, Electronic Structure and the Properties of Solids, Dover, Mineola, 1989, pp. 50–100.
[16] S.Y. Ren, J.D. Dow, Phys. Rev. B 45 (1992) 6492.
[17] B. Koiller, R. Osório, L.M. Falicov, Phys. Rev. B 43 (1991) 4170.
[18] A. Selloni, P. Marsella, R. Del Sole, Phys. Rev. B 33 (1986) 8885.

[19] L. Brey, C. Tejedor, Solid State Commun. 48 (1983) 403.
[20] L. Tsybeskov, S.P. Duttagupta, K.D. Hirschman, P. Fauchet, Appl. Phys. Lett. 68 (1996) 2058.
[21] G.E. Jellison, Optic. Mater. 1 (1992) 41.
[22] H.V. Nguyen, Y. Lu, S. Kim, M. Wakagi, R.W. Collins, Phys. Rev. Lett. 74 (1995) 3880.
[23] N. Koshida, H. Koyama, Y. Suda, Y. Yamamoto, M. Araki, T. Saito, K. Sato, Appl. Phys. Lett. 63 (1993) 2774.